

From boiling point to glass transition temperature: Transport coefficients in molecular liquids follow three-parameter scaling

B. Schmidtke, N. Petzold, R. Kahlau, M. Hofmann, and E. A. Rössler*

Universität Bayreuth, Experimentalphysik II, D-95440 Bayreuth, Germany

(Received 15 March 2012; revised manuscript received 3 August 2012; published 19 October 2012)

The phenomenon of the glass transition is an unresolved problem in condensed matter physics. Its prominent feature, the super-Arrhenius temperature dependence of the transport coefficients, remains a challenge to be described over the full temperature range. For a series of molecular glass formers, we combined $\tau(T)$ collected from dielectric spectroscopy and dynamic light scattering covering a range 10^{-12} s $< \tau(T) < 10^2$ s. Describing the dynamics in terms of an activation energy $E(T)$, we distinguish a high-temperature regime characterized by an Arrhenius law with a constant activation energy E_∞ and a low-temperature regime for which $E_{\text{coop}}(T) \equiv E(T) - E_\infty$ increases exponentially while cooling. A scaling is introduced, specifically $E_{\text{coop}}(T)/E_\infty \propto \exp[-\lambda(T/T_A - 1)]$, where λ is a fragility parameter and T_A a reference temperature proportional to E_∞ . In order to describe $\tau(T)$ still the attempt time τ_∞ has to be specified. Thus, a single interaction parameter E_∞ describing the high-temperature regime together with λ controls the temperature dependence of low-temperature cooperative dynamics.

DOI: [10.1103/PhysRevE.86.041507](https://doi.org/10.1103/PhysRevE.86.041507)

PACS number(s): 64.70.pm, 77.22.Gm, 78.35.+c

I. INTRODUCTION

Although of fundamental importance and extensively investigated, the glass transition phenomenon is far from being understood. Its most prominent feature is the super-Arrhenius temperature dependence of transport coefficients such as viscosity or correlation time τ , which is observed when a liquid is strongly supercooled. While a simple (molecular) liquid well above its melting point T_m exhibits a viscosity on the order of 10^{-3} Pa s, upon supercooling it may finally reach values of 10^{12} Pa s which are typical for solids. The corresponding temperature is defined as glass transition temperature T_g . The slowing down of dynamics is accompanied by only a slight and smooth change in structure. This has led to the interpretation that the glass transition is a kinetic transition and several theoretical approaches have been developed, yet none is fully accepted [1–4]. In particular, it remains a great challenge of any theory of the liquid state to provide an interpolation of $\tau(T)$, which covers the full range from the boiling point down to T_g .

Often the empirical Vogel-Fulcher-Tammann formula (VFT), $\lg \tau/\tau_\infty = D/(T - T_0)$, is applied to fit experimental data. One of the problems faced when applying VFT is that its parameters depend strongly on the fitting interval and it fails when relaxation data well above T_m are included. Regarding the divergence of the correlation time implied by VFT at $T_0 < T_g$, doubts have also been raised [5]. Numerous further formulas have been proposed attempting to fit $\tau(T)$, but none is fully satisfying. Another route of searching for “corresponding states” of liquids relies on scaling, for example, the low-temperature regime by introducing some crossover temperature [6–9]. Yet, in the different approaches the physical meaning of the crossover temperature is quite different, and it is difficult to extract unambiguously a crossover temperature.

Inspecting the experimental situation it turns out that, although extensively studied close to T_g , molecular glass

formers are not sufficiently well investigated in the high-temperature regime above T_m . With a few exceptions, most tests of interpolating $\tau(T)$ are restricted to time constants above about 10^{-9} s, actually ignoring a temperature range of up to 300 K until the high-temperature limit $\tau_\infty \cong 10^{-12}$ s is essentially reached. The most popular approach probing molecular reorientation is dielectric spectroscopy [10–12], but for technical reasons most such experiments do not cover frequencies above a few gigahertz. Correlation times down to 10^{-12} s are now easily available when glass formers are studied by depolarized dynamic light scattering (LS) using a tandem-Fabry-Perot interferometer (TFPI) and a double monochromator (DM) [13–17]. We have combined LS, including also photon correlation spectroscopy (PCS) data [17] measured up to 440 K of a series of 17 molecular liquids with the data obtained by dielectric spectroscopy, thus covering, in most cases, the entire temperature range needed to attempt a complete description of $\tau(T)$, i.e., which includes both the high- as well as the low-temperature regime of molecular liquids. As different rank reorientational correlation functions are probed by DS and LS, one expects some difference in the absolute values of $\tau(T)$, which, however, can be neglected on a logarithmic scale. For example, comparing $\tau(T)$ obtained from DS and LS, a factor of 1.65 among the time constant has been reported [16]. The time constants $\tau(T)$ are extracted from the DS and LS susceptibility spectra by standard line-shape analysis described in Refs. [10–13, 15, 17–19]. Looking for a minimal number of system-specific parameters controlling $\tau(T)$ in the range 10^{-12} – 10^2 s, we will show that actually three parameters are sufficient.

II. RESULTS

Figure 1(a) displays, in an Arrhenius representation, dielectric correlation times collected in our group (open symbols) [10, 15, 18–22] together with few other literature data for glycerol [11], benzophenone [23], salol [24], propylene carbonate [25], *n*-butyl benzene [26], and iso-propylene benzene [27, 28]. In addition, we have included our data together with previously published LS data [14–17] (full symbols)

*Corresponding author.

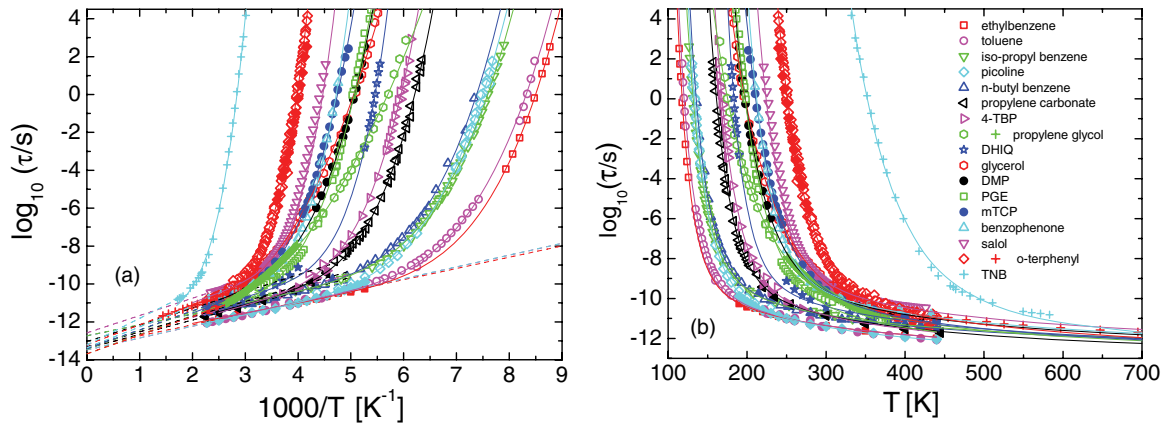


FIG. 1. (Color online) Reorientational correlation times of molecular liquids obtained by dielectric spectroscopy (open symbols) [10,18–21] and dynamic light scattering (full symbols) (this work and [14–17]); 4-TBP: 4-*tert*-butyl pyridine, DHIQ: decahydroisoquinoline, DMP: dimethyl phthalate, PGE: monoepoxide phenyl glycidyl ether, *m*-TCP: *m*-tricresyl phosphate; data for *n*-butyl benzene from [26,29], iso-propylene benzene from [27,28,35]; viscosity data for *o*-terphenyl [31], trisnaphthyl benzene (TNB) [33], and propylene glycol [34] (crosses); for toluene, ²H NMR data [36] have been included; straight dashed lines: high-temperature Arrhenius behavior; solid lines: full fit by Eqs. (1) and (3). Corresponding T_g values are listed in Table I.

together with literature LS data for *n*-butyl benzene [29]. In the cases of dimethyl phthalate (DMP) and *m*-tricresyl phosphate (*m*-TCP), we only use LS data as we collected both TFPI/DM and PCS data [30]. It is obvious that adding the LS data (solid symbols in Fig. 1) extends the temperature range significantly to be included in a full-scale description of $\tau(T)$, a fact better seen when the data are plotted as a function of temperature [Fig. 1(b)]. Even including the LS data, however, one reaches correlation times on the order of 10^{-12} s at our experimental high-temperature limit of 440 K only in the case of the low- T_g liquids (say, $T_g < 180$ K). For the systems with high T_g this limit is not reached. An exception is *o*-terphenyl ($T_g = 245$ K), for which viscosity data [31] are available up to almost 700 K, which is actually above the boiling point ($T_b = 605$ K) [32] and allows us to cover the high-temperature regime also for this high- T_g system. Here, with regard to our LS data measured up to 440 K, still another 260 K have to be covered to reach 10^{-12} s, finally. As another high- T_g system we included viscosity data of $\alpha\alpha\beta$ -trisnaphthyl benzene (TNB; $T_g = 343$ K) [33], additional data for propylene glycol [34], and iso-propylene benzene [35].

It is well known from transport data in low-viscosity (non-glass-forming) liquids that their temperature dependence is described by an Arrhenius law [37]. This may also be anticipated when inspecting the data in Fig. 1(a). At high temperatures a simple Arrhenius law appears to describe the data well, whereas the apparent activation energy $E(T)$ strongly increases at lower temperatures. The analysis of Stickel *et al.* [38] has shown that for molecular glass formers the Arrhenius regime has been reached by dielectric experiments in some cases. However, the analysis included only molecular rates below 10^{10} Hz, which is not always sufficient to reach the high-temperature range. In Fig. 2 we plot the apparent activation energy $E(T) = \partial \ln(\tau)/\partial(1/T)$ at the highest temperatures investigated as revealed by our LS data. Although some scatter shows up as a derivative is involved, in all cases the activation energy shows a trend to level off

at the highest temperatures. In the case of low- T_g liquids the Arrhenius behavior is well established over 100–200 K. For example, $E(T)$ is essentially constant above 200 K for ethyl benzene, while for *o*-terphenyl for which viscosity data are available up to the boiling point the Arrhenius behavior is observed only above 500 K. Regarding the nonfragile glass formers glycerol and propylene glycol, the Arrhenius regime is not clearly reached but again a trend toward $E(T) = E_\infty = \text{const.}$ is observed in both cases. This also holds for some other fragile high- T_g systems like salol. Thus, although we significantly extended the temperature range studied so far, only an estimate may be available for the activation energy E_∞ in some liquids. In order to facilitate estimating E_∞ in these cases, we assumed a pre-exponential time τ_∞ listed in Table I, which actually does not significantly vary for the considered liquids [cf. Fig. 1(b)]. Together with the experimental value of τ at highest temperatures, this allows some reasonable estimate of E_∞ for nonfragile glass formers. The optimization

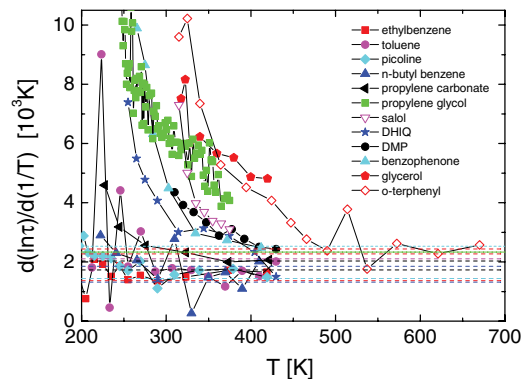


FIG. 2. (Color online) Apparent activation energy $E(T) = \partial \ln(\tau)/\partial(1/T)$ of the temperature dependence of $\tau(T)$ at highest temperatures, as revealed by light scattering. A trend of $E(T)$ to become constant is recognized; dashed lines indicate values of E_∞ used for the analysis (cf. Table I).

TABLE I. Parameters of the analysis: glass transition temperature T_g [defined by $\tau_\alpha(T_g) = 100$ s], high-temperature activation energy E_∞ , reference temperature T_A corresponding to the optimization, generalized fragility parameter λ , logarithm of pre-exponential factor τ_∞/s .

Sample	T_g [K]	E_∞ [K]	T_A [K]	λ	$\lg \tau_\infty/s$	T_A/T_g
Ethyl benzene	115	1369	128	7.67	-13.34	1.11
Toluene	117	1440	131	7.15	-13.49	1.12
<i>n</i> -Butyl benzene	131	1315	150	6.46	-12.74	1.15
Iso-propyl benzene	128	1342	145	6.44	-12.74	1.13
α -Picoline	129	1438	148	6.6	-13.47	1.15
Propylene carbonate	157	1729	177	7.04	-13.41	1.13
4- <i>tert</i> -Butyl pyridine (4-TBP)	164	1761	185	7.3	-13.30	1.13
Propylene glycol	168	2332	205	3.32	-13.69	1.22
Decahydroisoquinoline (DHIQ)	180	1851	201	7.37	-13.34	1.12
Glycerol	188	2271	235	3.56	-13.69	1.25
Dimethyl phthalate (DMP)	191	2029	221	5.66	-13.04	1.16
Monoepoxide phenyl glycidyl ether (PGE)	194	2321	215	7.08	-13.45	1.11
<i>m</i> -Tricresyl phosphate (m-TCP)	205	2301	235	6.21	-13.42	1.15
Benzophenone	207	2530	227	8.87	-13.37	1.10
Salol	218	2104	242	8.5	-12.58	1.11
<i>o</i> -Terphenyl	245	2441	274	8.26	-13.22	1.12
Trinaphthyl benzene (TNB)	343	3232	390	8.09	-13.22	1.14

procedure presented in the following takes specifically into account that E_∞ cannot be determined unambiguously in some of the liquids considered.

Although the energy E_∞ is an apparent quantity and must not be connected to some single-particle barrier in the liquid, we take the Arrhenius high-temperature dependence of $\tau(T)$ as an empirical fact and as a starting point of our analysis. Explicitly, we assume

$$\tau(T) = \tau_\infty \exp[(E_\infty + E_{\text{coop}}(T))/T], \quad (1)$$

where the apparent activation energy $E(T)$ is decomposed into a temperature-independent part E_∞ and a temperature-dependent part $E_{\text{coop}}(T)$. The quantity $E_{\text{coop}}(T)$ reflects the cooperative dynamics becoming dominant at low temperature, and its properties have been discussed by several authors [3,4,39–41]. The corresponding values E_∞ and τ_∞ are listed in Table I.

In Fig. 3(a), by plotting $T \lg(\tau/\tau_\infty) - E_\infty$ the quantity $E_{\text{coop}}(T)$ is displayed as a function of temperature. The high-temperature regime is now characterized by E_{coop} being essentially zero, while at low temperatures $E_{\text{coop}}(T)$ strongly increases for most liquids in a rather similar way, except for the nonfragile liquids glycerol and propylene glycol. In Fig. 3(b) $E_{\text{coop}}(T)$ is plotted on a logarithmic scale. Straight lines are observed for the low- T_g systems. In the case of the high- T_g systems and particularly for the nonfragile liquids, the curves bent over at low values of E_{coop} . Most probably this is due to an underestimated E_∞ . This once again points to the principal difficulty of determining E_∞ correctly. Moreover, we are faced with the problem of analyzing $E_{\text{coop}}(T)$ containing the error of a not-correctly-chosen E_∞ in addition to scatter reflecting experimental errors in $\tau(T)$. Regardless, we assume that $E_{\text{coop}}(T)$ is a simple exponential function of temperature; explicitly,

$$E_{\text{coop}}(T) \propto \exp[-\lambda(T/T_A - 1)]. \quad (2)$$

For reasons which will become clear below, we have introduced two parameters: a reference temperature T_A and a generalized fragility parameter λ which controls the “steepness” of $E_{\text{coop}}(T)$ in Fig. 3(b). Together with E_∞ and τ_∞ , four parameters are needed to describe the full temperature dependence of $\tau(T)$ in the present state of analysis, and so far we are free to choose any reference temperature T_A defining an “isoenergetic” point.

Here the question arises whether there is some connection between the reference temperature T_A and the high-temperature activation energy E_∞ . For this purpose we first reinspect Fig. 3(b). The quantity $E_{\text{coop}}(T = T_g)$, i.e., the energy at T_g , is higher, the higher T_g is. A trend already anticipated in Fig. 1(a). Indeed, the ratio $E_{\text{coop}}(T_g)/T_g$ appears to be roughly constant [cf. Fig. 4(a)], but this is not surprising as it follows from the definition of $T \lg(\tau/\tau_\infty) - E_\infty$, with E_∞ being a relatively small quantity. One may speculate whether $E_\infty \propto T_g$ holds. This is also checked in Fig. 4(a). Indeed, both ratios $E_{\text{coop}}(T_g)/T_g$ and E_∞/T_g appear to be constant, although some scatter/trend is observed. As T_g is an “isodynamic point” chosen arbitrarily, it is not expected to be a physically relevant temperature, but the correlation observed in Fig. 4(a) suggests that the temperature dependence of the low-temperature dynamics may be linked to the high-temperature activation energy E_∞ , explicitly $T_A \propto E_\infty$, and the four-parameter description $(\tau_\infty, E_\infty, \lambda, T_A)$ could possibly be reduced to a three-parameter description.

In order to find the relationship among T_A and E_∞ , we display the quantity $E_{\text{coop}}(T)/E_\infty$ as a function of the reduced temperature T/E_∞ in a semilogarithmic plot [cf. Fig. 4(b)]. Again, straight lines of different slopes are observed, suggesting that a common intersection exists possibly in the range $0.05 > T/E_\infty > 0.15$. Given the experimental uncertainty of E_∞ , this intersection may be smeared out. In order to find T_A in the range $T_g < T_A < E_\infty$, we take recourse to an optimization procedure. We fit $E_{\text{coop}}(T)$ in Fig. 3(a) for

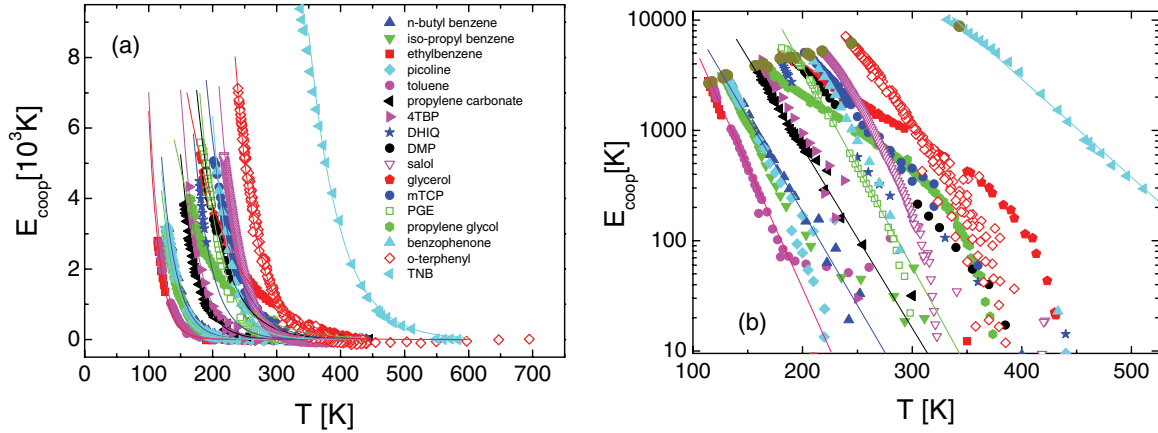


FIG. 3. (Color online) (a) Quantity $E_{\text{coop}}(T)$ [cf. Eq. (1)] as a function of temperature. (b) Data in a semilogarithmic plot; straight lines signal exponential dependence in particular for low- T_g liquids. Marked points indicate $E_{\text{coop}}(T_g)$. For high- T_g and nonfragile liquids the curves bent over at low E_{coop} values are probably due to an underestimated value of E_{∞} .

all systems by the expression

$$E_{\text{coop}}/E_{\infty} = a \exp \left[-\lambda \left(\frac{T}{bE_{\infty}} - 1 \right) \right], \quad (3)$$

where a and b are universal (global) parameters to be determined under the condition that the correlation between the experimental and fitted values of E_{∞} [by applying Eq. (3) to the data in Fig. 3(a)] becomes best. Our search yields the result that $E_{\text{coop}}(T_A) \cong E_{\infty}$ ($a \cong 1$) and $T_A \cong 0.104E_{\infty}$ ($b \cong 0.104$). The inset in Fig. 5(b) shows a satisfying correlation between the optimized E_{∞}^{opt} and the experimental values of E_{∞} , confirming our procedure. In Fig. 5(a) we show $E_{\text{coop}}(T)/E_{\infty}^{\text{opt}}$ vs $T/E_{\infty}^{\text{opt}}$, where the nonfragile liquids glycerol and propylene glycol show a significantly different behavior reflected by a much lower generalized fragility parameter λ . The values obtained for T_A and λ are included in Table I. One may call Fig. 5(a) [and Fig. 4(b)] a generalized Angell plot where reduced relaxation data [here $E_{\text{coop}}(T)/E_{\infty}$] are plotted vs reduced temperature T/E_{∞} instead of vs T/T_g , as in the original Angell plot [42]. In other words, the physically well

defined (but in some glass formers experimentally difficult to access) quantity E_{∞} defines the energy scale of the glass transition phenomenon.

In Fig. 5(b) a master curve is shown by plotting $E_{\text{coop}}(T)/E_{\infty}^{\text{opt}}$ vs $\lambda(T/T_A - A)$, i.e., the fragility parameter λ is taken to scale the reduced temperature axis. Indeed, all data can be collapsed to a single straight line. In Figs. 1(a) and 1(b) very satisfying three-parameter ($E_{\infty}, \lambda, \tau_{\infty}$) fits of $\tau(T)$ by Eqs. (1) and (3) are shown (using the universal parameters a and b), which cover all the available data essentially from the boiling point down to T_g .

III. DISCUSSION AND CONCLUSION

Concluding, we propose a three-parameter interpolation of the complete temperature dependence of transport quantities in molecular liquids which can be easily supercooled, i.e., when time constants in the range of 10^{-12} – 10^2 s are covered. Here one has to exclude diffusion data, as they show a “decoupling phenomenon” close to T_g [43]. The decomposition along Eq. (1) is not unique, and our sole justification is the success

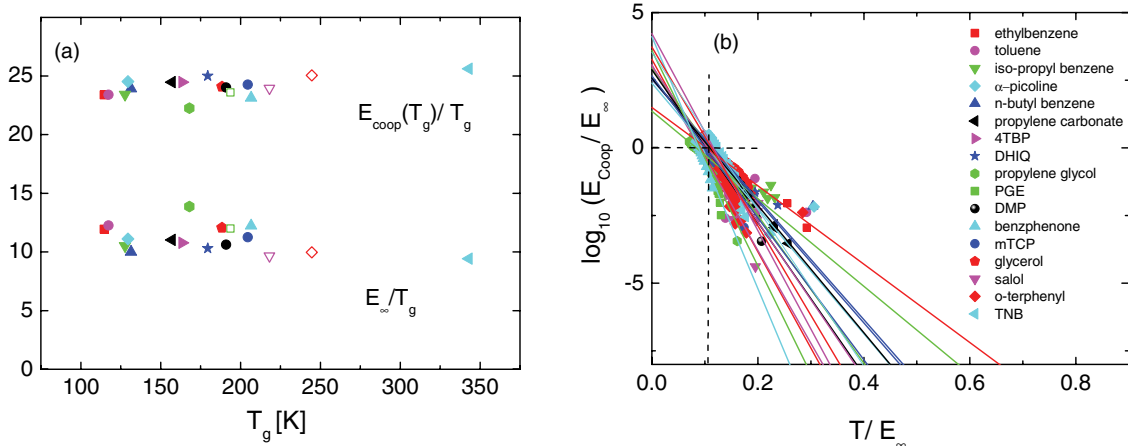


FIG. 4. (Color online) (a) Correlation between $E_{\text{coop}}(T = T_g)$ and E_{∞} , respectively, with the glass transition temperature T_g . (b) Reduced energy $E_{\text{coop}}(T)/E_{\infty}$ vs reduced temperature T/E_{∞} , dashed lines mark intersection after optimization [cf. Fig. 5(a)].

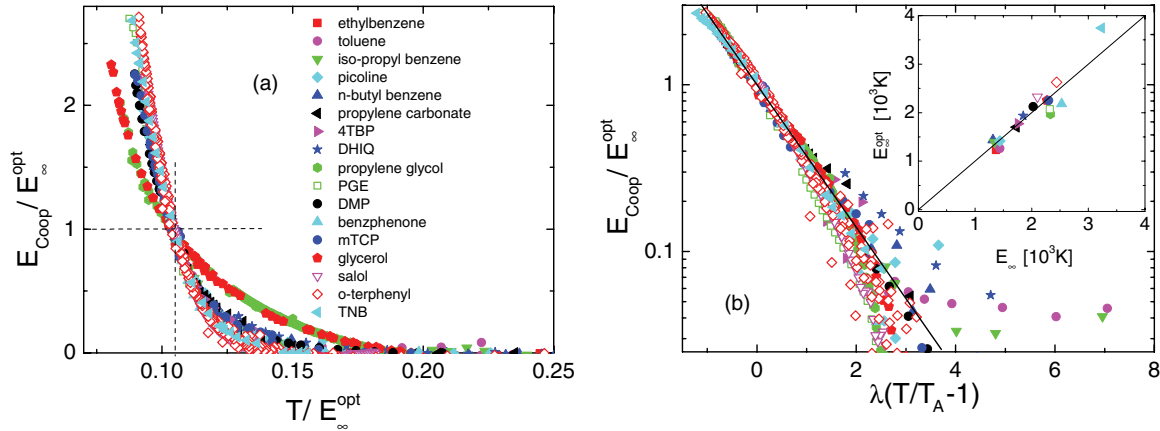


FIG. 5. (Color online) (a) $E_{\text{Coop}}/E_{\infty}^{\text{opt}}$ as a function of the reduced temperature $T/E_{\infty}^{\text{opt}}$ with E_{∞}^{opt} obtained by the optimization strategy (values of T_A and fragility parameter λ given in Table I). (b) Corresponding master curve obtained by introducing the fragility parameter λ and $T_A = 0.104 E_{\infty}^{\text{opt}}$ (cf. Table I); inset: correlation between E_{∞}^{opt} and the experimentally determined E_{∞} .

of the corresponding scaling, a minimal set of system-specific parameters, and furthermore, a simple exponential describes $E_{\text{Coop}}(T)$. We interpret the quantity E_{∞} extracted from the high-temperature transport data as an interaction parameter which, together with the single fragility parameter λ , controls the low-temperature behavior of $\tau(T)$. We emphasize that λ is defined by the “steepness” of $E_{\text{Coop}}(T/T_A)$ in contrast to the conventional fragility parameter m defined via $\tau(T/T_g)$. Thus, current attempts to relate m with some other physical properties have to be reconsidered.

We note a scaling of the kind of Eq. (3) was already proposed by the theoretical work of Kivelson, Tarjus, and co-workers [3,39–41] and a similar one by experimental studies [44]. Yet, to our knowledge, no one made a systematic study on a series of molecular liquids including high-temperature data which, as mentioned, have been rare. Important to note, the crossover temperature discussed by Kivelson *et al.* is connected to the presumable appearance of cooperative dynamics well above T_m (the so-called onset temperature), whereas the present T_A turns out to be right in the middle between T_g and T_m and thus possibly close to T_c of the mode coupling theory [2]. We note that, as an optimization procedure is applied, the universal parameters a and b depend on the quality of the experimental data, and actually, the optimization minimum is rather broad. As mentioned, attempts to scale the $\tau(T)$ data for glass formers have usually started from the low-temperature side; for instance, the time constants close to T_g have been collapsed to provide a single master curve by scaling out two parameters, namely, T_g and the fragility index m , and which works up to a crossover temperature which lies near $1.2T_g$ [7]. At higher temperatures individual curves

have been found, indicating that there a different transport mechanism takes over. In contrast, the present approach starts from the high-temperature side where an Arrhenius law is well documented, and again, a two-parameter scaling applies when the influence of the high-temperature dynamics is separated from the $\tau(T)$ data. In both cases a similar crossover temperature is disclosed. All in all, the present finding is of great relevance for the future theory of the glass transition phenomenon associated with the super-Arrhenius temperature dependence of the correlation time, which sets in well above the melting point and is thus an important feature of any liquid.

As we propose a universal description of $\tau(T)$ for molecular liquids, this also allows for some forecasts. For example, Capaccioli and Ngai [45] recently reiterated the controversy of providing a reliable estimate of T_g of water. They suggested $T_g = 136 \text{ K}$ as the best value. Taking this value for granted, we fitted our formula to the $\tau(T)$ data from [46], which the authors also used. In this way, we are able to extract the fragility parameter $\lambda = 2.6$ (referring to $m = 37$), which is close to that of glycerol and propylene glycol, both of which are nonfragile. As expected, water is a hydrogen bond network, forming liquid similar to glycerol and thus is not a fragile glass former. Actually, Capaccioli and Ngai estimated $m = 44$, which is in good agreement with our prediction.

ACKNOWLEDGMENTS

The authors thank D. Kruk, A. Bourdick, and B. Pötzschner for helpful discussions, and the financial support of Deutsche Forschungsgemeinschaft (DFG) through Projects RO 907/11 and RO 907/15 is appreciated.

[1] T. R. Kirkpatrick, D. Thirumalai, and P. G. Wolynes, *Phys. Rev. A* **40**, 1045 (1989).
 [2] W. Götze and L. Sjögren, *Rep. Prog. Phys.* **55**, 241 (1992).
 [3] G. Tarjus, S. A. Kivelson, Z. Nussinov, and P. Viot, *J. Phys.: Condens. Matter* **17**, R1143 (2005).
 [4] L. Berthier and G. Biroli, *Rev. Mod. Phys.* **83**, 587 (2011).

[5] T. Heckscher, A. I. Nielsen, N. B. Olsen, and J. C. Dyre, *Nat. Phys.* **4**, 737 (2008).
 [6] E. Rössler, *J. Chem. Phys.* **92**, 3725 (1990).
 [7] E. Rössler, K.-U. Hess, and V. Novikov, *J. Non-Cryst. Solids* **223**, 207 (1998).
 [8] E. J. Saltzmann and K. S. Schweizer, *J. Chem. Phys.* **121**, 2001 (2004).

- [9] Y. Elmatad, J. P. Garrahan, and D. Chandler, *J. Phys. Chem. B* **113**, 5563 (2009).
- [10] A. Kudlik, S. Benkhof, T. Blochowicz, C. Tschirwitz, and E. Rössler, *J. Mol. Struct.* **479**, 201 (1999).
- [11] P. Lunkenheimer, U. Schneider, R. Brand, and A. Loidl, *Contemp. Phys.* **41**, 15 (2000).
- [12] F. Kremer and A. Schönhal, *Broadband Dielectric Spectroscopy* (Springer, Berlin, 2003).
- [13] H. Z. Cummins, G. Li, Y. H. Hwang, G. Q. Shen, W. M. Du, J. Hernandez, and N. J. Tao, *Z. Phys. B* **103**, 501 (1997).
- [14] J. Wiedersich, N. V. Surovtsev, V. N. Novikov, E. Rössler, and A. P. Sokolov, *Phys. Rev. B* **64**, 064207 (2001).
- [15] S. V. Adichtchev, S. Benkhof, T. Blochowicz, V. N. Novikov, E. Rössler, C. Tschirwitz, and J. Wiedersich, *Phys. Rev. Lett.* **88**, 055703 (2002).
- [16] A. Brodin and E. A. Rössler, *Eur. Phys. J. B* **44**, 3 (2005).
- [17] N. Petzold and E. A. Rössler, *J. Chem. Phys.* **133**, 124512 (2010).
- [18] T. Blochowicz, Ch. Tschirwitz, St. Benkhof, and E. A. Rössler, *J. Chem. Phys.* **118**, 7544 (2003).
- [19] T. Blochowicz, A. Brodin, and E. A. Rössler, *Adv. Chem. Phys.* **133**, 127 (2006).
- [20] T. Blochowicz, C. Gainaru, P. Medick, C. Tschirwitz, and E. A. Rössler, *J. Chem. Phys.* **124**, 134503 (2006).
- [21] J. Hintermeyer, A. Herrmann, R. Kahlau, C. Goiceanu, and E. A. Rössler, *Macromolecules* **41**, 9335 (2008).
- [22] C. Gainaru, R. Kahlau, E. A. Rössler, and R. Böhmer, *J. Chem. Phys.* **131**, 184510 (2009).
- [23] P. Lunkenheimer, L. C. Pardo, M. Köhler, and A. Loidl, *Phys. Rev. E* **77**, 031506 (2008).
- [24] F. Stickel, E. W. Fischer, and R. Richert, *J. Chem. Phys.* **104**, 2043 (1996).
- [25] K. L. Ngai, P. Lunkenheimer, C. León, U. Schneider, R. Brand, and A. Loidl, *J. Chem. Phys.* **115**, 1405 (2001).
- [26] L. Andrussov, in *Eigenschaften der Materie in ihren Aggregatzuständen: Transport-Phänomene I*, Landolt-Börnstein II5a (Springer, Berlin, 1969).
- [27] A. I. Nielsen, T. Christensen, B. Jakobsen, K. Niss, N. B. Olsen, R. Richert, and J. C. Dyre, *J. Chem. Phys.* **130**, 154508 (2009).
- [28] C. Gangasharan and S. S. N. Murthy, *J. Chem. Phys.* **99**, 9865 (1993).
- [29] S. Wiebel, Doctoral thesis, Technische Universität München, 2003.
- [30] N. Petzold and E. A. Rössler (unpublished).
- [31] G. Friz, G. Kuhlbörsch, R. Nehren, and F. Reiter, *Atomkernenergie* **13**, 25 (1968).
- [32] *CRC Handbook of Chemistry and Physics*, 78th ed. (CRC Press, Boca Raton, FL, 1997).
- [33] D. J. Plazek and J. H. Magill, *J. Chem. Phys.* **45**, 3038 (1966).
- [34] Data from https://dow-answer.custhelp.com/app/answers/detail/a_id/7457/~propylene-glycols-viscosity-information, © Copyright The Dow Chemical Company (2011).
- [35] A. J. Barlow, J. Lamb, and A. J. Matheson, *Proc. R. Soc. London, Ser. A* **292**, 322 (1966).
- [36] E. Rössler and H. Sillescu, *Chem. Phys. Lett.* **112**, 94 (1984).
- [37] E. A. Moelwyn-Hughes, *Physikalische Chemie* (Thieme, Stuttgart, 1970).
- [38] F. Stickel, E. W. Fischer, and R. Richert, *J. Chem. Phys.* **104**, 2043 (1996).
- [39] Ch. Alba-Simionesco, D. Kivelson, and G. Trajus, *J. Chem. Phys.* **116**, 5033 (2002).
- [40] S. Sastry, *PhysChemComm* **3**, 79 (2000).
- [41] D. Kivelson, S. A. Kivelson, X. L. Zhao, Z. Nussinov, and G. Tarjus, *Physica A* **219**, 27 (1995).
- [42] C. A. Angell, in *Relaxation in Complex Systems*, edited by K. L. Ngai and G. B. Wright (US Dept. of Commerce, Springfield, 1985).
- [43] F. Fujara, B. Geil, H. Sillescu, and G. Fleischer, *Z. Phys. B* **88**, 195 (1992).
- [44] C. Dreyfus, A. Le Grand, J. Gapinski, W. Steffen, and A. Patkowski, *Eur. Phys. J. B* **42**, 309 (2004).
- [45] S. Capaccioli and K. Ngai, *J. Chem. Phys.* **135**, 104504 (2011).
- [46] G. Monaco, A. Cunsolo, G. Ruocco, and F. Sette, *Phys. Rev. E* **60**, 5505 (1999).